Structure and hydration free energy of ketone compound in neutral and cationic state by molecular dynamics simulation

MASASHI IWAYAMA, KAZUTOMO KAWAGUCHI, HIROAKI SAITO, HIDEMI NAGAO

Division of Mathematical and Physical Science, Graduate School of Natural Science and Technology,
Kanazawa University, Kakuma, Kanazawa 920-1192, Japan,
E-mail: iwayama@wriron1.s.kanazawa-u.ac.jp

Abstract. *Structure and hydration property of acetone and 3-pentaone in the neutral and cationic state were investigated by using molecular dynamics (MD) and free energy calculations. The force field parameters of stretching vibration, angle bending, and partial charges of each molecule in the neutral and cationic state were developed by using density functional theory (DFT) calculations with B3LYP method and 6-31+G** basis set. The optimized structures by using these force field parameters in gas phase were compared with the experimental data and AMBER force fields parameters (parm99). From the results, the optimized structure in the neutral state of acetone was in good agreement with the experimental data. The evaluated hydration free energy in the neutral state of acetone was closed to the experimental data, while that of 3-pentaone was little bit larger than the experimental data. The ionization effect of ketone molecule on the hydration free energies was found to be significant in both molecules.*

Keywords: Molecular Dynamics, Ketone Compound, Force Field, Geometry Optimization, Hydration Free Energy

1 Introduction

Redox reaction of organic molecules plays an important role in vivo. For instance, the redox reaction is related to the biological reactions such as the metabolism, photosynthesis, and intracellular signal transduction [1,2]. The redox potential is a key property to understand the mechanism of redox reaction of the molecule in solution. In the experiment, the redox potentials have been measured as the relative potential for the standard hydrogen electrode at room temperature. In the case of organic molecules, the observed redox potential of ketone molecule was in 0.12-0.20 eV [3]. On the other hand, the redox potentials of organic molecules have also been evaluated by using the quantum mechanics (QM) calculations and the combined quantum mechanics/molecular mechanics (QM/MM) methods [4,5]. In such calculations, the solvated snapshot structures of the molecule in the neutral and cationic (or anionic) state are taken to calculate the ionization potential and hydration free energy of the molecule. The redox potential is evaluated by the ionization potentials and the difference of the hydration free energies between each state. In these calculations, the hydration free energy was known to strongly depend on the solvated structure of the molecule [6]. Thus, the appropriate sampling of the solvated structure should be important for accurate calculation of the redox potential.

The molecular dynamics (MD) and Monte Carlo (MC) method have been used to take the snapshot structures of the solute in solution. In such simulation, the empirical force field has commonly used for the molecules in the system, and several force fields such as the CHARMM [7] and AMBER [8,9] have been developed so far. These force fields commonly consist of the bond stretching, angle bending, torsional energetics for the intramolecular potential and the coulomb and van der Waals (vdW) interactions for the intermolecular potential [10-14]. In the case of organic molecule, the OPLS [15] and AMBER force field have been adopted so far. In case of AMBER, the partial charges of the molecule are mainly calculated by the empirical scheme called AM1-BCC (bond charge correction) [18,19]. However, the restrained electrostatic potential (RESP) charge calculated by

a larger basis set should be adopted for more accurate electrostatic property of the molecules. The parm99 force field [16,17], which is a representative in the recent AMBER force field, presents the force field parameters of intramolecular potential. The torsion parameters were presented for small 82 organic molecules with the RESP charges by the density functional theory (DFT) calculations with B3LYP method and cc-PVDZ basis set. These parameters are determined to represent the smallest root mean square deviation (RMSD) compared with the experimental data, however, the torsion parameters for 11 hydrocarbons and 7 chlorides were evaluated with absolute errors in 0.1 kcal/mol relative to the experimental values. These intramolecular parameters are evaluated for the molecules in neutral state, but that of ionized molecules have not been presented yet. Thus, the force field parameters should be improved and developed for the sampling of the organic conformation in neutral and cationic (or anionic) state in solution.

In this study, we performed the DFT calculations with high-level basis set to obtain the optimized structures of acetone and 3-pentanone in the neutral and cationic state and developed new force field parameters for the stretching vibration, angle bending and partial charges of those molecules. We carried out the MD simulations of these models by using the optimized force field parameters and investigated the structure and hydration free energies of the molecules in neutral and cationic state. The ionization effect of these molecules on the hydration free energy was also examined in this study.

2 Computational Methods

2.1 Geometry Optimization in Gas Phase

Geometry optimizations of the acetone and 3-pentanone in the neutral and cationic states in gas phase were performed by DFT-B3LYP [20,21] calculations with 6-31+G** basis set [22-24]. The diffuse function was adopted for the ionized molecule to estimate the influence of extent of charge distribution [25]. In this study, the dependence of basis set on the total energy of the optimized structure was examined by using the various basis sets of 3-21G, 6-31G*, 6-31G**, 6-31+G*, 6-31+G**, 6-311G**, and 6-311+G**. The calculations of the 6-31G including the extended basis set such as the polarization function and the diffuse function showed lower energy than that with 3-21G basis set. The triple split valence basis sets showed even lower values. The differences of the minimum energies between in the neutral and cationic state were similar with that of the 6-31G in the each molecule. These calculations were done by Gaussian 03 [26].

2.2 Force Field

The force field for the intramolecular interaction of the molecule is represented as sum of the bond stretching, angle bending, and torsional energy as following equation,

$$V^{\text{intra}} = \sum_{\text{bonds}} K_r \left(r - r_{\text{eq}}\right)^2 + \sum_{\text{angles}} K_\theta \left(\theta - \theta_{\text{eq}}\right)^2 + \sum_{\text{dihedrals}} \frac{V_{ijkl}^n}{2}\left[1 + \cos\left(n\phi_{ijkl} - \gamma_{ijkl}\right)\right], \quad (1)$$

where K_r and K_θ are spring constants of the stretching and angle, r_{eq} and θ_{eq} are equilibrium bond lengths and angles, V_{ijkl}^n is the spring constant of torsional energy constructed by $ijkl$, n is the phase period, and γ_{ijkl} is equilibrium torsion angle, respectively.

The parameters of equilibrium length and angle of the molecules were obtained from the optimized structure by B3LYP/6-31+G** calculation, and the spring and bending parameters were determined by fitting these parameters to reproduce the potential energy curve which is obtained by DFT calculations with different bond distance and angle of the molecule. For the evaluation of spring and vending constants, 5 sample data were taken in this study.

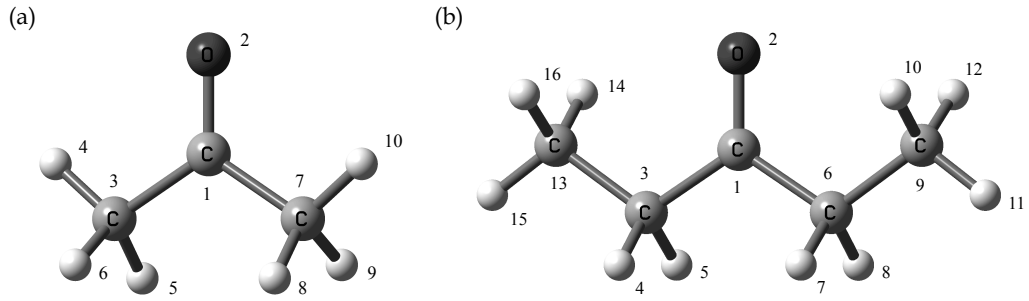

Figure 1. Optimized structures for neutral state of (a) acetone and (b) 3-pentanone from DFT-B3LYP /6-31+G** calculations.

Table 1. Relative spring constants (kcal/mol/Å²) and equilibrium bond lengths (Å) for parm99 force field, DFT calculations, and experimental data of acetone and 3-pentanone.

	parm99[a]		neutral state		cation state		Exptl[b]
bond	K_r	r_{eq}	K_r	r_{eq}	K_r	r_{eq}	r_{eq}
			acetone				
O2–C1	570.0	1.229	932.3	1.219	806.8	1.214	1.213
C3–C1	317.0	1.522	295.8	1.518	251.0	1.524	1.520
H4–C3	340.0	1.090	394.4	1.091	394.4	1.089	1.103
H5–C3	340.0	1.090	376.5	1.096	376.5	1.095	1.103
H6–C3	340.0	1.090	376.5	1.097	376.5	1.098	1.103
C7–C1	317.0	1.522	295.8	1.518	251.0	1.524	1.520
H8–C7	340.0	1.090	376.5	1.096	376.5	1.096	1.103
H9–C7	340.0	1.090	376.5	1.097	376.5	1.098	1.103
H10–C7	340.0	1.090	394.4	1.091	394.4	1.089	1.103
			3-pentanone				
O2-C1	570.0	1.229	927.8	1.219	950.2	1.192	
C3–C1	317.0	1.522	286.9	1.525	179.3	1.573	
H4–C3	340.0	1.090	358.6	1.100	376.5	1.095	
H5–C3	340.0	1.090	358.6	1.100	358.6	1.101	
C6–C1	317.0	1.522	286.9	1.525	179.3	1.573	
H7–C6	340.0	1.090	358.6	1.100	358.6	1.101	
H8–C6	340.0	1.090	358.6	1.100	376.5	1.095	
C9–C6	310.0	1.526	322.7	1.528	322.7	1.518	
H10–C9	340.0	1.090	385.5	1.094	394.4	1.092	
H11–C9	340.0	1.090	376.5	1.095	376.5	1.097	
H12–C9	340.0	1.090	385.5	1.094	394.4	1.093	
C13–C3	310.0	1.526	322.7	1.528	317.5	1.518	
H14–C13	340.0	1.090	385.5	1.094	394.4	1.092	
H15–C13	340.0	1.090	376.5	1.095	376.5	1.097	
H16–C13	340.0	1.090	385.5	1.094	394.4	1.093	

[a] The parm99 force field parameters from Ref. 16 and 17.
[b] Experimental values for structural parameters of acetone by microwave spectroscopy from Ref. 35.

Table 2. Relative spring constants (kcal/mol/deg²) and equilibrium bond angles (deg) of parm99 force field, results of DFT calculations, and experimental data for acetone and 3-pentanone.

	parm99[a]		neutral state		cation state		Exptl[b]
angle	K_θ	θ_{eq}	K_θ	θ_{eq}	K_θ	θ_{eq}	θ_{eq}
			acetone				
C3-C1-O2	80.0	120.4	80.0	121.6	33.8	119.0	
H4-C3-C1	50.0	109.5	65.7	110.1	68.8	111.4	
H5-C3-C1	50.0	109.5	63.6	110.7	63.2	107.1	
H6-C3-C1	50.0	109.5	62.2	109.8	60.3	106.0	
C7-C1-O2	80.0	120.4	80.0	121.6	33.8	119.0	
C7-C1-C3	63.0	117.0	57.7	116.8	48.0	122.0	116.0
H8-C7-C1	50.0	109.5	63.6	110.7	63.2	107.1	
H9-C7-C1	50.0	109.5	62.2	109.8	60.3	106.0	
H10-C7-C1	50.0	109.5	65.7	110.1	68.8	111.4	
			3-pentanone				
C3-C1-O2	80.0	120.4	84.0	121.8	41.5	122.0	
H4-C3-C1	50.0	109.5	67.7	107.6	67.7	104.6	
H5-C3-C1	50.0	109.5	67.7	107.6	62.8	101.2	
C6-C1-O2	80.0	120.4	84.0	121.8	41.5	122.0	
C6-C1-C3	63.0	117.0	61.5	116.4	47.0	115.9	
H7-C6-C1	50.0	109.5	67.7	107.6	62.8	101.2	
H8-C6-C1	50.0	109.5	67.7	107.6	62.8	104.6	
C9-C6-C1	63.0	111.1	106.9	114.2	87.3	114.8	
H10-C9-C6	50.0	109.5	72.6	111.0	72.6	112.3	
H11-C9-C6	50.0	109.5	67.7	110.5	62.8	106.9	
H12-C9-C6	50.0	109.5	72.6	111.0	72.6	112.2	
C13-C3-C1	63.0	111.1	106.9	114.2	87.3	114.8	
H14-C13-C3	50.0	109.5	72.6	111.0	72.6	112.3	
H15-C13-C3	50.0	109.5	67.7	110.5	62.8	106.9	
H16-C13-C3	50.0	109.5	72.6	111.0	72.6	112.2	

[a] The parm99 force field parameters from Ref. 16 and 17.
[b] Experimental values for structural parameters of acetone by microwave spectroscopy from Ref. 35.

Intermolecular interaction for the vdW and coulomb interaction are represented by following equation,

$$V^{\text{inter}} = \sum_{i\in I}^{\text{atoms}} \sum_{j\in J}^{\text{atoms}} \varepsilon_{ij} \left[\left(\frac{r_{ij}^e}{R_{ij}} \right)^{12} - 2 \left(\frac{r_{ij}^e}{R_{ij}} \right)^{6} \right] + \sum_{i\in I}^{\text{atoms}} \sum_{j\in J}^{\text{atoms}} \frac{q_i q_j}{\varepsilon R_{ij}}, \tag{3}$$

where ε_{ij} is the Lennard-Jones (L-J) parameter between atom i and j, r_{ij}^e is the equilibrium internuclear distance, which presents the minimum of potential energy as a function of atom distance R_{ij}, q_i is the effective point charge of atom i, and ε is the relative permittivity, respectively. The L-J parameters between different atoms are assigned as an arithmetic average for r_{ij}^e and geometric mean for ε_{ij} by the rule of Lorentz-Berthelot. All parameters of $r_{ij}^e/2$ and ε_{ij} are taken from the parm99

Table 3. RESP charge by DFT-B3LYP/6-31+G** for acetone and 3-pentanone

	neutral	cation		neutral	cation		neutral	cation
				acetone				
C1	0.621	0.506	H5	0.069	0.175	H9	0.069	0.175
O2	-0.535	-0.015	H6	0.069	0.175	H10	0.069	0.175
C3	-0.251	-0.272	C7	-0.251	-0.272			
H4	0.069	0.175	H8	0.069	0.175			
				acetone				
C1	0.530	0.391	H7	0.005	0.109	C13	-0.052	-0.098
O2	-0.517	-0.082	H8	0.005	0.109	H14	0.020	0.087
C3	-0.023	-0.035	C9	-0.052	-0.098	H15	0.020	0.087
H4	0.005	0.109	H10	0.020	0.087	H16	0.020	0.087
H5	0.005	0.109	H11	0.020	0.087			
C6	-0.023	-0.035	H12	0.020	0.087			

force field. The partial charges of the molecule were determined by the Merz-Singh-Kollman method [27] with B3LYP/6-31+G** calculations.

2.3 Molecular Dynamics Simulations

The MD simulations for the neutral and cationic state of the acetone and 3-pentanone were carried out with the parameters listed in Table 1, 2 and 3. The intramolecular torsion angles are constrained with harmonic potential to sample the structure around the potential energy minimum of the molecule. The spring constants for the constraints of torsion angle are determined by fitting these parameters to reproduce the potential energy curve, which is obtained by B3LYP/6-31+G** calculations. The MD simulations were carried out by AMBER 11 program packages. Langevin thermostat and barostat were used to control the system temperature (T = 300 K) and pressure (P = 1 atm) [28]. The acetone and 3-pentanone were solvated by 1425 water molecules in a cubic box with 39.8 Å × 37.4 Å × 38.0 Å and 1790 water molecules in a box with 44.5 Å × 39.3 Å × 39.5 Å, respectively. The TIP3P model [29] was adopted for water molecule. Particle Mesh Ewald (PME) method [30] was adopted for the calculation of coulomb interactions. Cut off lengths for the coulomb and vdW interactions were 12 Å. A time step for the MD calculations was 2.0 fs. The bond lengths including the hydrogen atoms were constrained by SHAKE method [31].

Energy minimization was performed with constraints of the heavy atoms of solute with 50 kcal/mol/Å² spring constant. MD calculations were carried out in the constant NPT condition, and then, system temperature was gradually increased from 100 K to 300 K for 100 ps. After that, NPT simulations were performed in which the constraints of solute were gradually reduced to zero for 100 ps. Finally, the equilibrium NPT-MD simulations were carried out for 10 ns.

Hydration Free Energy. We estimate the hydration free energy to investigate the solvation properties of the acetone and 3-pentanone in the neutral and cationic sate. The energy representation (ER) method was adopted for the estimation of hydration free energy in this study. In the ER method, the hydration free energy can be presented as an energy distribution functions $\rho^e(\varepsilon)$, $\rho_0^e(\varepsilon)$, and a correlation function $\chi_0^e(\varepsilon,\eta)$. The energy distribution $\rho^e(\varepsilon)$ is defined using energy coordinate and expressed by following equation;

$$\rho(\varepsilon) = \left\langle \sum_i \delta\left(v(\psi, \mathbf{x}_i) - \varepsilon\right) \right\rangle, \tag{4}$$

where ψ is the solute coordinate, $\mathbf{x}_i$ is the coordinate of i-th solvent molecule, respectively. The sum is taken over all the solvent molecules, and the energy distribution is obtained by the ensemble average. The energy distribution $\rho_0^e(\varepsilon)$ and the correlation function $\chi_0^e(\varepsilon,\eta)$ are constructed by inserting the solute molecule in the pure solvent system. The actual form of the hydration free energy and the details of the computations are presented elsewhere [32-34].

The calculation of the hydration fee energy requires two MD simulations for solution system and pure solvent system. The NVT-MD simulations of 300 ps for the solution system and that of 100 ps for the pure solvent system were carried out to obtain the distribution functions $\rho^e(\varepsilon)$ and $\rho_0^e(\varepsilon)$. The solute was treated as rigid molecule in water solvent in both simulations. The system coordinate was dumped every 10 fs for the solution system and 1 ps for the pure solvent system. The solute molecule was randomly inserted 1000 times into the pure solvent system. Finally the energy distribution function $\rho^e(\varepsilon)$ was estimated with 30k samples and $\rho_0^e(\varepsilon)$ with 100k samples.

3 Results and discussion

3.1 Optimized Structures in Gas Phase

The optimized structure (bond lengths and angles) of the acetone and 3-pentanone of the neutral and cationic state in gas phase calculated by DFT-B3LYP/6-31+G** were listed in Table 1 and 2 with the parm99 force filed parameters. In the neutral state, the bond lengths and angles of both molecules estimated by the DFT calculation were in good agreement with those of the param99. The differences of bond lengths between the param99 and DFT calculations were in ~0.01 Å. The differences of angles were shown to be ~3.1 degree in the 3-pentanone. However, because the estimated angles were obtained by large basis set (6-31+G**) in comparison with that used in the development of the param99, the predicted structures in this study should be more accurate. The optimized structure of acetone in the neutral state was compared with the experimental data in the gas phase. The differences of bond lengths and angles with the experimental data were ~0.012 Å and ~0.8 degree, respectively, showing an excellent agreement with experiment.

In the case of comparison with those in cationic state, the differences of bond lengths and angles between in neutral and cationic state were ~0.48 Å and ~6.4 degree, respectively. This large angle change in the cationic state should be due to the change of molecular orbital by ionization of the molecule; the change of molecular polarization should influence the intramolecular interaction between the atoms in the molecule, resulting in the change of molecular structure.

In our models, the DFT calculation showed that the total energies of acetone and 3-pentanone in gas phase were -5,256.55 eV and -7,396.33 eV in the neutral state and -5,246.97 eV and -7,387.13 eV in the cationic state, respectively. By way of comparison, the experimental data of first adiabatic ionization potential in gas phase are 9.69 eV for acetone and 9.32 eV for 3-pentanone [36]. The calculated ionization potentials of the acetone and 3-pentaone were 9.58 eV and 9.19 eV, being in good agreement with experimental data.

The partial charges of atoms in each molecule are listed in Table 3. To assesse the validity of these partial charges, the dipole moments of acetone and 3-pentanone in the neutral and cationic states, which were calculated by the classical method using the partial charges, were compared with those by the quantum chemical calculation and experimental data in Table 4. The calculated dipole moments using the RESP charges were evaluated by using the snapshots taken from the MD

Table 4. Comparison of dipole moment (debye) of DFT-B3LYP/6-31+G** and average in classical MD for acetone and 3-pentanone

molecule	state	DFT-B3LYP/6-31+G**	Classical/MD	Exptl[a]
acetone	neutral	3.19	3.21 ± 0.09	2.88 ± 0.03
	cation	2.12	2.54 ± 0.12	
3-pentanone	neutral	2.89	2.88 ± 0.05	2.82
	cation	2.30	2.48 ± 0.06	

[a] Experimental data from Ref. 36.

simulation in the equilibrium condition. The dipole moments by both quantum chemical and MD simulations were found to be in good agreement with the experimental data in both molecules.

3.2 Hydration Free Energy

The hydration free energies of acetone and 3-pentanone were estimated by the ER method with 39 snapshots for acetone and 31 snapshots for 3-pentanone in equilibrium state. The results were listed in Table 5. The standard deviations of the hydration free energies were 0.14 kcal/mol in the neutral state and 2.68 kcal/mol in the cationic state. The hydration free energy of 3-pentanone was larger than that of acetone, showing larger hydrophobicity of the 3-pentanone. This should be due to the addition of the hydrocarbons at the end of acetone molecule. The similar hydration character can be shown in the experimental data (see. in Table 5). The estimated hydration free energy for 3-pentanone was shown to be larger than the experimental data. This could be due to the constraints of torsion angle in the 3-pentanone; because of the constraints of the torsion angle, the molecular conformations, which have better affinity with conformations of surrounding water molecules, could not be sampled in the MD simulation, resulting in the larger hydration free energy of the 3-pentanone. There could be a possibility that the hydrophobicity of the added methyl group was overestimated due to the improper L-J parameters, which is transferred from param99. The improvement of the force field parameters and simulations condition should be done for more accurate estimation; this would be our future work.

The energy distributions of $\rho^{e}(\varepsilon)$ and $\rho_0^{e}(\varepsilon)$ for the neutral and cationic state in both molecules are plotted in Figure 2. In the energy distribution in neutral state, the distribution peak, which is caused by the hydrogen bonds with the surrounding water molecules, appears near -5 kcal/mol. The number of hydrogen bonds in the cationic state was explicitly larger than those in the neutral state, showing that the attractive interactions between the positively charged solute and surrounding water molecule in the solution become strong. The resultant hydration free energies of the acetone and 3-pentanone in the cationic state were shown to be much lower (~30 kcal/mol) than those in the neutral state. We can thus conclude that the these molecules in cationic state are stable in water solvent, and

Table 5. Hydration Free Energy (kcal/mol) for acetone and 3-pentanone

molecule	state	Calc	Exptl[a]
acetone	neutral	-2.34 ± 0.14	-3.80
	cation	-34.65 ± 2.74	
3-pentanone	neutral	-0.54 ± 0.13	-3.41
	cation	-28.25 ± 2.62	

[a] Experimental results of hydration free energies for organic molecules at 25 ℃ from Ref. 37.

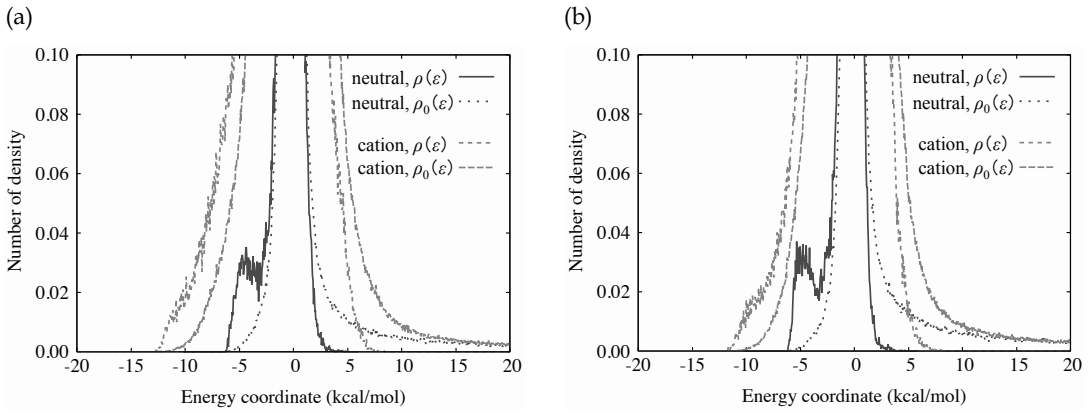

Figure 2. The energy distribution functions $\rho^e(\varepsilon)$ and $\rho_0^e(\varepsilon)$ for neutral and cation state of (a) acetone and (b) 3-pentanone with number of density on a snapshot in solution.

the ionization effect of ketone molecule on the hydration free energies is significant in both molecules.

4 Summary

We studied the structure and hydration property of the acetone and 3-pentaone in the neutral and cationic state by using molecular dynamics (MD) and free energy calculations. The force field parameters of the bond vibration, angle bending, and intramoleclular partial charges for the acetone and 3-pentanone were newly developed by the density functional theory (DFT) calculations with the B3LYP method and 6-31+G** basis set. The optimized structures of both molecules were in good agreement with the experimental data. The determined partial charges of these molecules reproduce the dipole, which is in good agreement with experimental data. Also the evaluated ionization potentials were consistent with the experimental data in ~0.13 eV errors. The hydration free energies of each molecule in the neutral and cationic state were estimated by energy representation (ER) method. The estimated hydration free energy of acetone in neutral state was close to the experimental data while that of the 3-pentanone was larger than the experimental data. This difference could be caused by constraints of the torsion angles of 3-pentanone. The observed hydration free energies of the acetone and 3-pentanone in the cationic state were shown to be much lower (~30 kcal/mol) than those in the neutral state, showing that the ionization effect of ketone molecule on the hydration free energies should be significant in both molecules.

References

[1] B. Alberts, A. Johnson, J. Lewis, M. Raff, K. Roberts, and P. Walter (2002), *Molecular Biology of the Cell*, Garland Science, 4 edition.

[2] V. Adler, Z. Yin, K. D. Tew, and Z. Rona (1999), Role of redox potential and reactive oxygen species in stress signaling, *Oncogene.*, **18**, 6104 – 6111.

[3] R. H. Baker and H. Adkins (1940), Oxidation Potentials of Ketones and an Aldehyde, *J. Am. Chem. Soc.*, **62**, 3305 - 3314.

[4] H. M. Senn, and W. Thiel (2009), QM/MM Methods for Biomolecular Systems, *Angew Chem Int Ed.*, **48**, 1198 – 1229.

[5] M. Cascella, A. Magistrato, I. Tavernelli, P. Carloni, and U. Rothlisberger (2006), Role of protein frame and solvent for the redox properties of azurin from *Pseudomonas aeruginosa*, *Proceedings of the National Academy of Sciences*, **103**, 19641 – 19646.

[6] Q. Shao and S. Jiang (2013), Effect of Carbon Spacer Length on Zwitterionic Carboxybetaines, *J. Phys. Chem. B.*, **117**, 1357 – 1366.

[7] A. D. MacKerell, Jr., D. Bashford, M. Bellott, R. L. Dunbrack, Jr., J. D. Evanseck, M. J. Field, S. Fischer, J. Gao, H. Guo, S. Ha, D. Joseph-McCarthy, L. Kuchnir, K. Kuczera, F. T. K. Lau, C. Mattos, S. Michnick, T. Ngo, D. T. Nguyen, B. Prodhom, W. E. Reiher, III, B. Roux, M. Schlenkrich, J. C. Smith, R. Stote, J. Staub, M. Wtanabe, J. Wiorkiewicz-Kuczera, D. Yin, and M. Karplus (1998), All-Atom Empirical Potential for Molecular Modeling and Dynamics Studies of Proteins, *J. Phys. Chem. B.*, **102**, 3586 – 3616.

[8] Y. Duan, C. Wu, S. Chowdhury, M. C. Lee, G. Xiong, W. Xhang, R. Yang, P. Cieplak, R. Luo, T. Lee, J. Caldwell, J. Wang, and P. Kollman (2003), A Point-Charge Force Field for Molecular Mechanics Simulations of Proteins Based on Condensed-Phase Quantum Mechanical Calculations, *J. Comp. Chem.*, **24**, 1999 – 2012.

[9] J. Wang, R. M. Wolf, J. W. Caldwell, P. A. Kollman, and D. A. Case (2004), Development and Testing of a General Amber Force Filed, *J. Comp. Chem.*, **25**, 1157 – 1174.

[10] S. J. Weiner, P. A. Kollman, D. A. Case, U. C. Singh, C. Ghio, G. Alagona, S. Profeta, Jr., and P. Weiner (1984), A New Force Field for Molecular Mechanical Simulation of Nucleic Acids and Proteins, *J. Am. Chem. Soc.*, **106**, 765 - 784.

[11] W. D. Cornell, P. Cieplak, C. I. Bayly, I. R. Gould, K. M. Merz, Jr., D. M. Ferguson, D. C. Spellmeyer, T. Fox, J. W. Caldwell, and P. A. Kollman (1995), A Second Generation Force Field for the Simulation of Proteins, Nucleic Acids, and Organic Molecules, *J. Am. Chem. Soc.*, **117**, 5179 - 5197.

[12] S. L. Mayo, B. D. Olafson, and W. A. GoddardⅢ (1990), DREIDING: A Generic Force Field for Molecular Simulations, *J. Phys. Chem.*, **94**, 8897 - 8909.

[13] A. T. Hagler, E. Huler, and S. Lifson (1974), Energy Functions for Peptides and Proteins. I . Derivation of a Consistent Force Field Including the Hydrogen Bond from Amide Crystals, *J. Am. Chem. Soc.*, **96**. 5319 - 5327.

[14] S. Lifson, A. T. Hagler, and P. Dauber (1974), Consistent Force Field Studies of Intermolecular Forces in Hydrogen-Bonded Crytstals. 1. Carboxylic Acids, Amides, and the C=O⋯H-Hydrogen Bonds, *J. Am. Chem. Soc.*, **101**, 5111 - 5121.

[15] W. L. Jorgensen, D. S. Maxwell, and J. Tirado-Rives (1996), Development and Testing of the OPLS All-Atom Force Field on Conformational Energetics and Properties of Organic Liquids, *J. Am. Chem. Soc.*, **118**, 11225 – 11236.

[16] S. J. Weiner, and P. A. Kollman (1986), An All Atom Force Field for Simulations of Proteins and Nucleic Acids, *J. Comp. Chem.*, **7**, 230 – 252.

[17] J. Wang, P. Cieplak, and P. A. Kollman (2000), How Well Does a Restrained Electrostatic Ptential (RESP) Model Perform in Calculating Conformational Energies of Organic and Biological Molecules?, *J. Comp. Chem.*, **21**, 1049 – 1074.

[18] A. Jakalian, B. L. Bush, D. B. Jack, and C. I. Bayly (2000), Fast, Efficient Generation of High-Quality Atomic Charges. AM1-BCC Model: I. Method, *J. Comp. Chem.*, **21**, 132 – 146.

[19] A. Jakalian, D. B. Jack, and C. I. Bayly (2002), Fast, Efficient Generation of High-Quality Atomic Charges. AM1-BCC Model: II. Parameterization and Validation, *J. Comp. Chem.*, **23**, 1623 – 1641.

[20] A. D. Becke (1993), A new mixing of Hartree-Fock and local density-functional theories, *J. Chem. Phys.*, **98**, 1372 – 1377.

[21] C. Lee, W. Yang, and R. G. Parr (1988), Development of the Colle-Salvetti correlation-energy formula into a functional of the electron density, *Phys. Rev. B.*, **37**, 785 – 789.

[22] P. C. Hariharan, and J. A. Pople (1973), The Influence of Polarization Functions on Molecular Orbital Hydrogenation Energies, *Theor. Chim. Acta. (Berl).*, **28**, 213 – 222.

[23] J. D. Dill, and J. A. Pople (1975), Self – consistent molecular orbital methods. XV. Extended Gaussian – type basis sets for lithium, beryllium, and boron, *J. Chem. Phys.*, **62**, 2921 – 2922.

[24] G. W. Spitznagel, T. Clark, J. Chandrasekhar, and P. V. R. Schleyer (1982), Stabilization of methyl anions by first-row substituents. The superiority of diffuse function-augmented basis sets for anion calculations, *J. Comp. Chem.*, **3**, 363 – 371.

[25] T. Clark, J. Chand rasekhar, G. W. Spitznagel, and P. V. R. Schleyer (1983), Efficient diffuse function-augmented basis sets for anion calculations. III. The 3-21+G basis sets for first-row elements, Li-F, *J. Comp. Chem.*, **4**, 294 – 301.

[26] M. J. Frisch, G. W. Trucks, H. B. Schlegel, G. E. Scuseria, M. A. Robb, J. R. Cheeseman, J. A. Montgomery, Jr., T. Vreven, K. N. Kudin, J. C. Burant, J. M. Millam, S. S. Iyengar, J. Tomasi, V. Barone, B. Mennucci, M. Cossi, G. Scalmani, N. Rega, G. A. Petersson, H. Nakatsuji, M. Hada, M. Ehara, K. Toyota, R. Fukuda, J. Hasegawa, M. Ishida, T. Nakajima, Y. Honda, O. Kitao, H. Nakai, M. Klene, X. Li, J. E. Knox, H. P. Hratchian, J. B. Cross, V. Bakken, C. Adamo, J. Jaramillo, R. Gomperts, R. E. Stratmann, O. Yazyev, A. J. Austin, R. Cammi, C. Pomelli, J. W. Ochterski, P. Y. Ayala, K. Morokuma, G. A. Voth, P. Salvador, J. J. Dannenberg, V. G. Zakrzewski, S. Dapprich, A. D. Daniels, M. C. Strain, O. Farkas, D. K. Malick, A. D. Rabuck, K. Raghavachari, J. B. Foresman, J. V. Ortiz, Q. Cui, A. G. Baboul, S. Clifford, J. Cioslowski, B. B. Stefanov, G. Liu, A. Liashenko, P. Piskorz, I. Komaromi, R. L. Martin, D. J. Fox, T. Keith, M. A. Al-Laham, C. Y. Peng, A. Nanayakkara, M. Challacombe, P. M. W. Gill, B. Johnson, W. Chen, M. W. Wong, C. Gonzalez, and J. A. Pople, Gaussian 03, Revision D.02; Gaussian, Inc., Wallingford CT, 2004.

[27] B. H. Besler, K. M. Merz, and P. A. Kollman (1990), ATOMIC CHARGES DERIVED FROM SEMIEMPIRICAL METHODS, *J. Comp. Chem.*, **11**, 431 – 439.

[28] S. E. Feller, Y. Zhang, R. W. Pastor, and B. R. Brooks (1995), Constant pressure molecular dynamics simulations: The Langevin piston method, *J. Chem. Phys.*, **103**, 4613 – 4621.

[29] W. L. Jorgensen, J. Chandrasekhar, J. D. Madura, R. W. Impey, and M. L. Klein (1983), Comparison of simple potential functions for simulating liquid water, *J. Chem. Phys.*, **79**, 926 – 935.

[30] T. Darden, D. York, and L. Pederson (1993), Particle mesh Ewald: An N · log(N) method for Ewald sums in large systems, *J. Chem. Phys.*, **98**, 10089 – 10092.

[31] G. J. Martyna (1994), Constant pressure molecular dynamics algorithms, *J. Chem. Phys.*, **101**, 4177 – 4189.

[32] N. Matubayasi, and M. Nakahara (2000), Theory of solutions in the energetic representation. I. Formulation, *J. Chem. Phys.*, **113**, 6070 – 6081.

[33] N. Matubayasi, and M. Nakahara (2002), Theory of solutions in the energy representation. II. Functional for the chemical potential, *J. Chem. Phys.*, **117**, 3605 – 3616.

[34] N. Matubayasi, and M. Nakahara (2003), Theory of solutions in the energy representation. III. Treatment of the molecular flexibility, *J. Chem. Phys.*, **119**, 9686 – 9702.

[35] T. Iijima, Zero-point Average Structure of a Molecular Containing Two Symmetric Internal Rotors. Acetone, *Bull. Chem. Soc. Jpn.*, **45**, 3526 – 3530.

[36] D. R. Lide (2004), *CRC Handbook of Chemistry and Physics*, CRC Press.

[37] J. Wang, W. Wang, S. Huo, M. Lee, and P. A. Kollman (2001), Solvation Model Based on Weighted Solvent Accessible Surface Area, *J. Phys. Chem. B.*, **105**, 5055 – 5067.